



Persistence of iron limitation in the western subarctic Pacific SEEDS II mesoscale fertilization experiment

Mark L. Wells^{a,*}, Charles G. Trick^b, William P. Cochlan^c, Ben Beall^d

^a School of Marine Sciences, University of Maine, Orono, ME 04469-5741, USA

^b Schulich School of Medicine and Dentistry, Departments of Biology and Microbiology & Immunology, University of Western Ontario, London ON N6A 5B7, Canada

^c Romberg Tiburon Center for Environmental Studies, San Francisco State University, Tiburon, CA 94920-1205, USA

^d Department of Biology, University of Western Ontario, London ON N6A 5B7, Canada

ARTICLE INFO

Topical issue on "SEEDS II: The Second Subarctic Pacific Iron Experiment for Ecosystem Dynamics Study." The issue is compiled and guest-edited by the North Pacific Marine Science Organization (PICES) and International SOLAS.
Available online 3 July 2009

Keywords:

Iron
Iron limitation
Fertilization
Ligands
Phytoplankton
Physiological health
Incubation studies
Subarctic Pacific

ABSTRACT

The cumulative evidence from more than a dozen mesoscale iron-enrichment studies in high nitrate low chlorophyll (HNLC) waters demonstrates that iron limitation is widespread and very likely affects atmospheric carbon dioxide and thus global climate. However, the responses of microphytoplankton (>20 μm), predominantly diatoms, vary greatly among these mesoscale experiments even though similar amounts of iron were added, making it difficult to quantitatively incorporate iron effects into global climate models. Nowhere is this difference more dramatic than between the massive bloom observed during Subarctic Pacific Iron Experiment for Ecosystem Dynamics Study (SEEDS) I and the order of magnitude smaller ecosystem response in SEEDS II; two mesoscale experiments performed in the same HNLC region of the western subarctic Pacific in different years. Deckboard incubation experiments initiated during the early, middle, and late stages of the 32-day SEEDS II experiment show that while the two iron infusions increased phytoplankton growth, diatoms remained significantly limited by iron availability, despite total dissolved Fe concentrations in the patch being well above the diffusion-limited threshold for rapid diatom growth. This iron limitation was apparent <6 days after the initial iron infusion and was not alleviated by the second, smaller iron infusion. In contrast, smaller phytoplankton (<20 μm) showed a more restricted response to further iron amendments, indicating that their iron nutrition was near optimal. Iron complexed to desferrioximine B, a commonly available siderophore produced by at least one marine bacterium, was poorly available to diatoms throughout the patch evolution, indicating that these diatoms lacked the ability to induce high-affinity iron uptake systems. These results suggest that the strong organic complexation of Fe(III) observed in the SEEDS II-fertilized patch was not compatible with rapid diatom growth. In contrast, iron associated with protoporphyrin IX, a weaker iron complexing ligand of a class hypothesized to be representative of recycled iron species, was readily available to diatoms. Our findings demonstrate that a persistence of iron limitation was the primary factor underlying the comparatively small diatom response during SEEDS II. This continued growth limitation would have increased the importance of mesozooplankton grazing as a controlling factor in the SEEDS II ecosystem response.

© 2009 Elsevier Ltd. All rights reserved.

1. Introduction

Iron limitation and its effects on phytoplankton growth and carbon export in high nitrate, low chlorophyll (HNLC) regions are well recognized. A number of key commonalities characterize ecosystem responses in the 12 mesoscale enrichment studies conducted to date (~0.6 d⁻¹; de Baar et al., 2005), as well as with natural iron enrichments associated with island formations that pierce HNLC surface waters (Blain et al., 2001). Most notably it is the diatoms, often pennate species of the genus *Pseudo-nitzschia*,

that respond disproportionately to the alleviation of iron limitation and thus comprise the major component of phytoplankton biomass generated from iron infusion to surface waters (de Baar et al., 2005). These mesoscale experiments generally match the results of deckboard, bottle incubation experiments that also show intensified diatom growth with increased iron availability (Boyd et al., 1996; Leblanc et al., 2005; Martin and Fitzwater, 1988; Timmermans et al., 2001). But unlike bottle incubations, replication of the complex and logistically challenging mesoscale experiments at the same location is notably lacking. One exception was IronEx II in the equatorial Pacific where two iron-enriched patches were created, the second one using significantly less iron; but only limited intercomparison was possible between these experiments due to single vessel operational limitations

* Corresponding author. Tel.: +1 207 581 4322; fax: +1 207 581 4388.
E-mail address: mlwells@maine.edu (M.L. Wells).

(Coale et al., 1996). The general absence of experiment replication is problematic because although broad ecosystem responses among mesoscale experiments are similar in different oceanic regions, the biomass generated differs substantially (Boyd et al., 2007; de Baar et al., 2005). These large discrepancies make it difficult to quantitatively incorporate iron effects into ocean biogeochemical and global climate models.

The major exception to the replication problem are the Subarctic Pacific Iron Experiment for Ecosystem Dynamics Study (SEEDS) I and II; both experiments performed in early summer in the same region of the western subarctic Pacific but on different years (2001 and 2004, respectively). Despite the broadly similar oceanographic conditions observed during the two experiments, the biogeochemical outcomes were radically disparate (Tsuda et al., 2003, 2007). SEEDS I generated the largest increase in phytoplankton production of any mesoscale enrichment experiment to date, despite having only a single, pulsed iron infusion (Tsuda et al., 2003), whereas the ecosystem response during SEEDS II was an order of magnitude less despite roughly twice the amount of iron being added in two infusions (see Tsuda et al., 2009). This unexpected outcome highlights our very limited understanding of the mechanistic response of the ecosystem to iron input, and specifically which factors regulate the magnitude of this response. It also raises doubt about whether increased natural iron inputs, normally much smaller than used in these artificial manipulations, can generate the large ecosystem responses necessary to significantly affect atmospheric CO₂ and global climate (Martin, 1990).

It is critical that the factors responsible for the different ecosystem responses distinguishing SEEDS II from SEEDS I be identified if we are to gain predictive insights into the role of iron in marine biogeochemistry and global climate. There are two primary possibilities: iron was not the dominant limiting factor during SEEDS II, or iron limitation of the large eukaryotic phytoplankton (i.e., diatoms) was not alleviated by the two, large-scale iron additions. Although total iron concentrations indeed were significantly elevated in the iron-infused patch during SEEDS II (Nishioka et al., 2009), the chemical speciation of Fe(III) in seawater is known to be dominated by complexation with a comparatively stronger (L_1) and comparatively weaker (L_2) classes of functionally specific Fe(III) organic ligands (Gledhill and van den Berg, 1994; Powell and Donat, 2001; Rue and Bruland, 1995; Witter et al., 2000). The L_1 class ligands are believed to comprise siderophores released by prokaryotes while L_2 class ligands may represent planktonic molecular debris comprising intact or partially degraded intracellular metabolic constituents or surface-associated iron transporters released by grazing, viral lysis, or other mechanisms (e.g., see Sunda, 2001).

These organic Fe(III) chelators normally are present in seawater at concentrations in excess of dissolved iron (Berg, 1995; Croot and Johansson, 2000; Cullen et al., 2006; Powell and Donat, 2001; Rue and Bruland, 1995; Witter et al., 2000), and consideration of their effect on iron availability to marine microbes, both prokaryotic and eukaryotic, is essential for interpreting the outcome of iron-fertilization experiments. It is expected that a major fraction of infused iron in mesoscale experiments rapidly becomes complexed by these free ligand molecules. It is proposed that the relative availability of iron in the stronger and weaker ligand classes differ substantially among prokaryotic and eukaryotic phytoplankton, with prokaryotes accessing iron in the stronger ligand class while eukaryotic phytoplankton utilize iron from the weaker ligand class (Hutchins et al., 1999b). More recent studies suggest that eukaryotic organisms may be capable of inducing high-affinity iron uptake systems that indeed can take up iron associated with siderophores (Maldonado and Price, 1999; Salmon et al., 2006; Shaked et al., 2005; Wells et al., 2005), but

very few studies have examined these effects in natural systems, and particularly in oceanic HNLC waters.

We present results of three deckboard incubation studies performed sequentially during the course of the 32-day SEEDS II mesoscale iron-enrichment study. These experiments tested two related hypotheses. First, large eukaryotic phytoplankton (diatoms) remained iron limited despite elevated total iron concentrations in the fertilized patch, and second, although iron complexed by weaker ligands may be used readily by diatoms, iron bound to strong organic chelators (siderophores) remains poorly available to diatoms. If both hypotheses test true, the second hypothesis would provide indirect evidence for the mechanism causing restricted diatom growth; a pool of Fe that is relatively unavailable to large eukaryotic phytoplankton. The two chelators tested were desferrioxamine B (DFB), a known bacterial and fungal siderophore (Crumbliss, 1991; Martinez et al., 2001), and protoporphyrin IX (PIX), a porphyrin ring believed to be representative of metabolic ligands recycled and released to seawater (Hutchins et al., 1999b). The response to these chelators was measured over the course of the SEEDS II iron-induced bloom to evaluate whether phytoplankton adapted over time to better utilize these chelated forms of iron (Wells et al., 2005) and to assess how the ecosystem would respond to further iron additions as a function of the degree and duration of iron stress in the patch.

2. Materials and methods

Sampling was conducted during a 6-week oceanographic cruise in 2004 to the western subarctic Pacific Ocean aboard the RV *Kilo Moana*. Surface seawater was collected for the deckboard incubation experiments at three times over the 32-day SEEDS II experiment from within the core of the iron-enriched patch, as determined by nightly SF₆ mapping during the early to mid time scales after the initial enrichment, or by chlorophyll mapping during the latter stages of the experiment. The sampling dates were July 26, and August 4 and 13, which corresponded to Days 6, 15 and 24 after the initial Fe enrichment (Fig. 1).

An all-Teflon[®] sampling system was used to collect surface waters for incubation. The system, comprising a plastic towfish with Kevlar-incased Teflon[®] (PFA) tubing and double diaphragm pump, has been demonstrated to provide clean water (Roy and

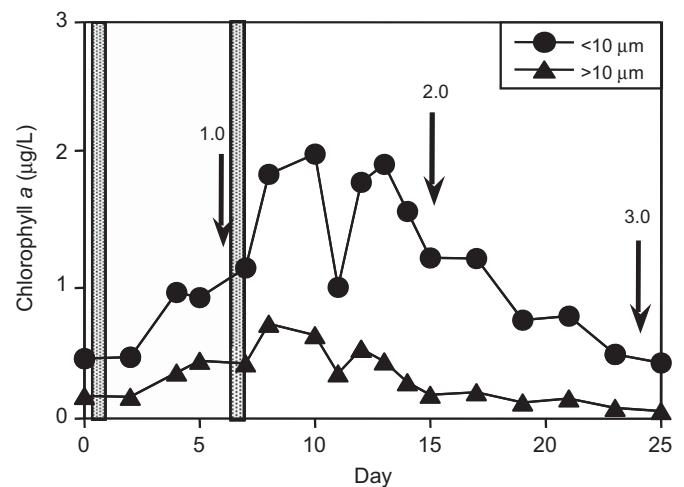


Fig. 1. Temporal changes in the relative composition of size-fractionated (<10 µm and >10 µm) chlorophyll-*a* concentration inside the iron-enriched patch during SEEDS II (as measured aboard the R.V. *Hakuho Maru*). Shaded areas indicate the day of the 1st and 2nd iron-enrichment periods, and arrows indicate the initiation of the Early, Middle and Late Bloom deckboard incubation experiments. (Data kindly provided by H. Saito.)

Wells, 2008) without significant impacts on even the fragile components of the ecosystem (e.g., micrograzers—E. Lessard, unpublished data). The towfish was positioned 8 m outboard of the vessel using the ship's crane to avoid contamination associated with the vessel. The pumped seawater was directed onboard while the vessel maintained headway (1–2 knots), and into a shipboard fabricated, positive pressure clean room, where it was dispensed under a Class 100 HEPA bench. A three-way valve assembly at the point of sampling allowed the system to be flushed continuously at 4 L min⁻¹ for 30 min before and during the bottle rinsing and sampling stages.

Seawater samples were pumped continuously from 10 m depth (~50% light level), and coarse sieved through 200- μ m, pre-rinsed nylon mesh (Nitex) to remove mesozooplankton, as these organisms have a disproportionately large and variable impact on phytoplankton production in the bottles. To reduce potential effects from small-scale surface patchiness during sample collection, a 50-L acid-cleaned polyethylene carboy was filled, mixed thoroughly and samples subsequently dispersed into acid-cleaned and rinsed 10-L polycarbonate carboys for treatment and incubation.

Three duplicate treatments and controls were prepared; Fe(III) enrichment (3 nM added), Fe(III)-DFB enrichment (3:3.3 nM Fe(III):DFB) and Fe(III)-PIX enrichment (3:3.3 nM Fe(III):PIX), whereas controls were unamended with either macronutrients or micronutrients. The Fe(III)-ligand mixtures were premixed to minimize the precipitation of Fe(III) oxyhydroxides by bubbling freshly collected seawater (30 mL) with filtered CO₂ gas to achieve pH < 6 before the sequential addition of ligand followed by Fe(III). The solution then was re-equilibrated to pH 8 by bubbling with filtered air, thus ensuring that no colloidal oxyhydroxides were present in the stocks at the time of culture enrichment. Some sorption of PIX to the bottle wall was observed during this process, so these treatments likely had somewhat lower total Fe(III)-PIX concentrations than the Fe(III) and Fe(III)-DFB treatments. The stability of these ligands in the cultures was not measured directly, though Fe(III)-DFB is stable over time with respect to photochemical degradation (Barbeau et al., 2003) and biological impact (Hutchins et al., 1999a; Wells, 1999).

The duplicate treatments and controls were placed within clear Plexiglas[®] deck incubators maintained at the sea-surface temperature and photosynthetic photon flux density (PPFD) attenuated to ca. 50% of incident surface flux (using neutral density screening and blue Plexiglas sheeting). This light level was similar to the irradiance where the incubation water and initial cell populations were collected. The carboys remained sealed until the end of the experiment, but were subsampled daily by compressed air overpressure, as described in Coale (1991). Separate subsamples of treatment and control samples were filtered in parallel through glass-fiber (Whatman[®] GF/F; nominal pore size = 0.7 μ m) and membrane (Poretics; 20- μ m pore size) filters over the 4–8-day experiments for determination of size-fractionated chlorophyll *a*, nutrients, flow cytometric community analysis, and species composition. For chlorophyll, duplicate samples (50–100 mL) for each size fraction were filtered in parallel onto the two different pore-sized filters, and extracted in the dark for > 24 h in 8 mL of *N,N*-dimethylformamide (DMF) at -20 °C (Suzuki and Ishimaru, 1990). The fluorescence readings were subsequently measured following a non-acidification protocol (Welschmeyer, 1994) using a Turner Designs model 10-AU fluorometer calibrated at the beginning of the cruise with pure chlorophyll *a* (Sigma Chemical) following standard JGOFS protocols (Knap et al., 1996). Macronutrients (nitrate+nitrite, silicic acid and ortho-phosphate) were collected in pre-cleaned polypropylene tubes, and analyzed with a Lachat QuikChem 8000 Flow Injection Analysis system using standard colorimetric techniques

(Knepel and Bogren, 2002; Smith and Bogren, 2001; Wolters, 2002).

Flow cytometry was used to examine the phytoplankton and heterotrophic prokaryote communities. Phytoplankton were classified into three size groups: phytoeukaryotes ~2–6 μ m (hereafter referred to as small nanoeukaryotes), ~6–15 μ m (large nanoeukaryotes), and cyanobacteria. The presence of chain-forming diatoms complicated the enumeration of larger (>15 μ m) phytoplankton. The largest chains were beyond the sensitivity range of the instrument, and chain-elongating growth of smaller chains would not be detected adequately by measuring particle abundance. However, the majority of cells within this >15- μ m category were captured as microphytoplankton on the >20- μ m filter and thus are included in our chlorophyll *a* analyses.

Flow cytometry samples were analyzed without fixative within 2 h of collection using a FACSCalibur flow cytometer equipped with a blue (488 nm) laser and orange (585/42 nm bandpass) and red (650 nm long pass) detectors (Becton-Dickinson, CA, USA). Samples not analyzed immediately were stored at ~4 °C in the dark until analysis. All data acquisitions were done using logarithmic signal amplification. Cytometer sample flow rates were calibrated using bead stocks of known concentration (Calibrite beads, Becton-Dickinson, CA, USA) and particle size was calibrated using beads of known size (Flow Cytometry Size Bead Kit, Invitrogen). Eukaryotic phytoplankton were distinguished by size and red fluorescence (instrument settings: Foward Scatter = E-01, and FL3 = 350). Cyanobacteria were identified by size, and red and orange fluorescence (instrument settings: Foward Scatter = E00, FL2 = 280, and FL3 = 350). *Prochlorococcus* were identified by their size and red fluorescence, but were present in low numbers and are not considered in these analyses. Heterotrophic bacterioplankton were stained for enumeration with the nucleic acid stain SYBR Green I (Invitrogen) (Marie et al., 1997). The abundance of nanoeukaryotes and cyanobacteria was calculated from acquisition duration, the number of events, and instrument flow rate.

The smaller components of the phytoplankton community, including cyanobacteria and nanoeukaryotes, did not exhibit batch culture exponential growth as expected in incubation-type experiments presumably due to grazing effects, and perhaps also the dynamics of interspecies competition (nanoeukaryotes). Rather than cell numbers, we therefore used chlorophyll-derived growth rates as the primary means to compare responses among treatments. While this approach also suffers from grazing complications, plus the effects from changing cellular chlorophyll *a* concentrations, it provides a more integrative estimate of the community response to the metal treatments and allows direct comparison between the small and large phytoplankton size fractions. Net growth rates (μ) were determined in each replicate treatment or control bottle according to

$$\mu = \frac{\ln(N_1/N_0)}{t_1 - t_0}$$

where N_1 and N_0 are the chlorophyll *a* concentrations at time 1 (t_1) and time 0 (t_0), respectively.

Linear mixed modelling by the NLME module in R (The R Project for Statistical Computing; www.r-project.org) was used to analyze the changes in biomass for each of the measures in the incubation experiments: community (GF/F) chlorophyll *a* concentration, microphytoplankton (>20 μ m) chlorophyll *a* concentration, small and large nanophytoplankton abundance, cyanobacterial abundance, and heterotrophic prokaryotic abundance. The statistical model for each experiment considered the effects of Day, Treatment for differences in overall biomass among the treatments, and the interaction between Day and Treatment

as the effect of treatment on growth. The analysis of treatment effects in the statistical analysis are presented as contrasts of the effect of treatment on growth against the Day and Treatment term for the control treatment and the reported probability is based on a *t*-test of the contrast coefficient (West et al., 2007). The repeated-measures experimental design was included in the model by a random intercept and day effect for each bottle. The maximum likelihood model-fitting approach used in the NLME module permits unbalanced designs due to missing data, which was the case in the incubation experiments since some biomass data were not available. The statistical model was constructed as outlined in West et al. (2007), using likelihood ratio tests of models constructed using unrestricted maximum likelihood algorithms and parsimony. The statistical significance of contrasts between the growth in the treatments and the growth in the controls was calculated by the NLME package in R.

3. Results

3.1. Growth in the control bottles

Details of the *in situ* response of the planktonic ecosystem to iron enrichments are provided in companion papers in this special issue. The time-dependent changes in size-fractionated (<10 μm, >10 μm) chlorophyll concentrations in the fertilized patch are shown in Fig. 1, along with the days that the three replicate deckboard incubations were initiated. Incubation experiments were timed to evaluate the *in situ* community response shortly after the initial iron fertilization (Early Bloom), near the bloom maximum (Middle Bloom), and during the late decline of the iron-induced bloom (Late Bloom).

Chlorophyll *a* biomass increased exponentially in the control bottles of both the Early Bloom and the Middle Bloom experiments, as expected for in-patch waters, given the alleviation of iron limitation and a reduction of grazing pressure by the removal of mesozooplankton (Fig. 2). However, chlorophyll-determined growth rates differed slightly between these controls, with the growth rate in the Early Bloom control ($0.37 \pm 0.11 \text{ d}^{-1}$) being slightly higher than that in the Middle Bloom incubation ($0.16 \pm 0.10 \text{ d}^{-1}$), which had a delayed growth response. Spot measurements of dissolved iron concentrations in the bottles showed no evidence of bottle contamination (data not shown). The community (GF/F) estimated growth rate in the Early Bloom

control within the range of in-patch growth rates estimated from dilution experiments ($\sim 0.3 \text{ d}^{-1}$; Tsuda et al., 2009). Total chlorophyll *a* biomass in controls of the Late Bloom incubation increased only slightly over the 4-day duration (Fig. 2). The Late Bloom incubation was terminated after 4 days because flowing seawater incubator temperatures began to increase during the ship transit to port.

The size-fractionated growth response among experimental controls was more variable. Chlorophyll-derived growth rates of smaller phytoplankton (<20 μm) were markedly higher ($0.29 \pm 0.01 \text{ d}^{-1}$) in the Early Bloom experiment control than in the Middle ($0.02 \pm 0.03 \text{ d}^{-1}$) and Late Bloom ($0.01 \pm 0.09 \text{ d}^{-1}$) incubations (Figs. 3B, 4B, 5B). In contrast, the growth rates of microphytoplankton (>20 μm), microscopically observed to be dominated by diatoms, were $1.02 \pm 0.07 \text{ d}^{-1}$, $0.81 \pm 0.12 \text{ d}^{-1}$, and $0.55 \pm 0.12 \text{ d}^{-1}$ in the control bottles of the Early, Middle, and Late Bloom incubations, respectively (Fig. 3A, 4A, 5A). These findings contrast with the *in situ* phytoplankton response to iron enrichment, where the <10-μm size fraction was observed to obtain higher levels of chlorophyll *a* biomass than the >10-μm size fraction (Fig. 1).

Flow cytometric analyses showed the small nanoeukaryotes (2–6 μm) exhibited significant positive growth in the control only in the Late Bloom experiment (Fig. 5D; linear mixed model, experiment-specific growth term, $p < 0.001$), while growth in the Middle Bloom experiment was significantly negative (Fig. 4D; linear mixed model, experiment-specific growth term, $p < 0.001$). There are no data for the small nanoeukaryotes during the first stages of Early Bloom experiment due to instrument problems but the growth trend during the last 2 days also was negative (Fig. 3D). Cyanobacteria grew significantly only in the Middle Bloom experiment (Fig. 4C; linear mixed model, experiment-specific growth term, $p < 0.001$). The abundance of heterotrophic prokaryotes did not change significantly in any of the incubation experiments (data not shown).

3.2. The effect of further Fe additions

Supplementing the surface waters of the fertilized patch with additional Fe(III) (3 nM) increased growth in most treatments, though the response differed between the large- and small-sized fractions. The statistical models for chlorophyll-derived growth showed no significant positive effects for Fe(III) addition on the entire phytoplankton community in the Early Bloom experiment, initiated 6 days after the first SEEDS II *in situ* iron enrichment, but total chlorophyll *a* (>GF/F) was enhanced significantly by Fe(III) addition in the Middle Bloom ($p < 0.05$, linear mixed model contrast (LMMC); sum of Fig. 4A,B) and Late Bloom ($p < 0.001$, LMMC; sum of Fig. 5A,B) experiments. Fe(III) addition had no effect on chlorophyll *a* in the smaller (<20 μm) phytoplankton size class during the Early Bloom experiment (Fig. 3B) but increased by 10-fold the chlorophyll-derived growth rates of smaller (<20 μm) phytoplankton in the Middle Bloom experiment ($0.20 \pm 0.04 \text{ d}^{-1}$ vs. $0.02 \pm 0.03 \text{ d}^{-1}$), generating chlorophyll *a* concentrations twice that in the controls by Day 6 (Fig. 4B). A more limited response of the small phytoplankton was observed in the Late Bloom experiment, where Fe(III) addition resulted in short-lived increases in chlorophyll *a* concentrations (Fig. 5B).

Flow cytometric analyses of cell numbers of cyanobacteria and small and large nanoeukaryotes illustrated the complexities underlying the bulk community response to Fe(III). In the Early Bloom incubation, cyanobacteria abundance decreased steadily with time by 4-fold in step with that measured in the control (Fig. 3E). The numbers of large nanoeukaryotes (6–15 μm) increased in the Fe(III) treatment, though growth was significantly

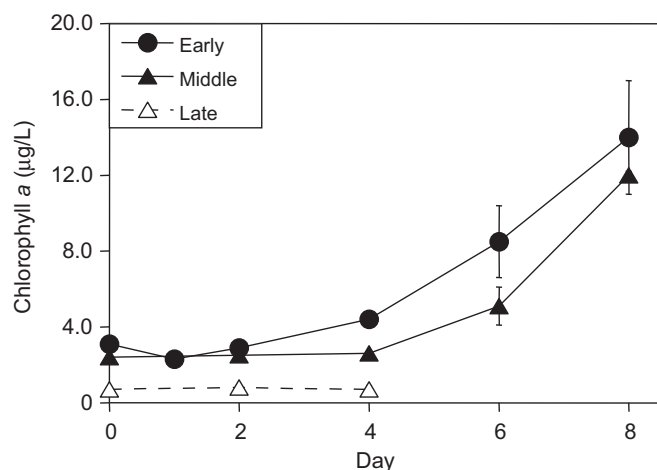


Fig. 2. Total (GF/F) chlorophyll *a* concentration as a function of time in the control (un-amended) bottles during the three, deckboard incubation experiments. Each symbol represents the mean \pm range of duplicate samples; no error bars indicate the errors are smaller than the width of the symbol.

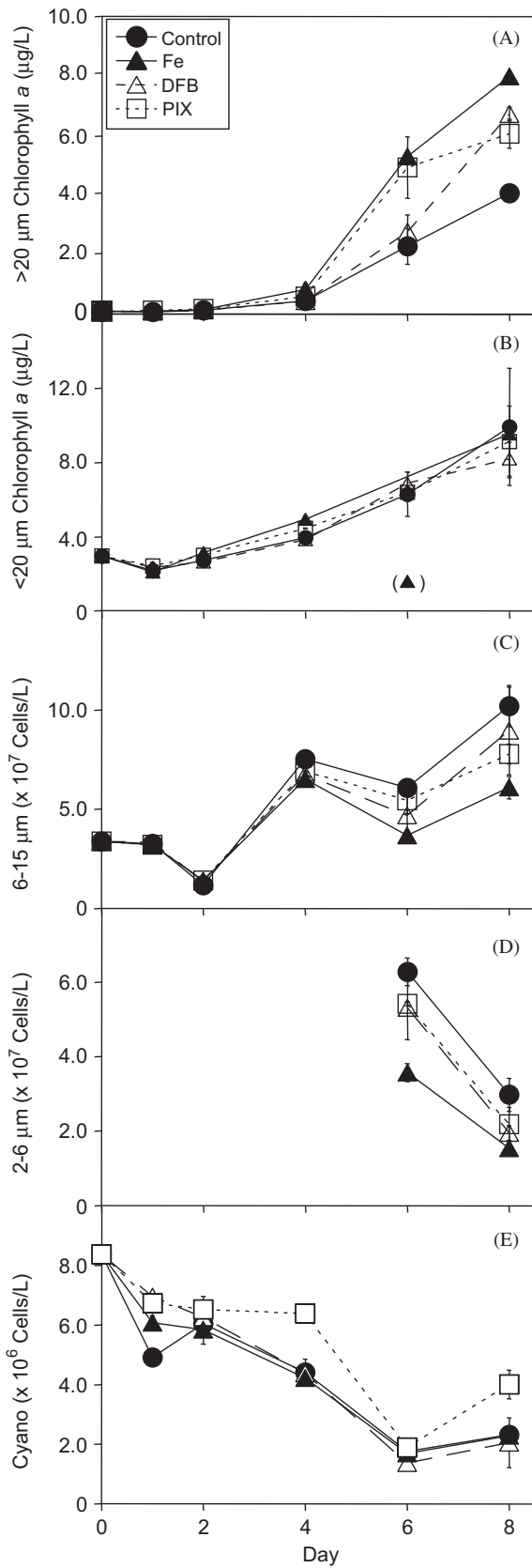


Fig. 3. The size-fractionated growth response to iron and Fe(III)-ligand amendments during the Early Bloom incubation experiment (July 26, 2004) for >20- μm phytoplankton (A), <20- μm phytoplankton (B), large (6–15 μm) nanoeukaryotes (C), small (2–6 μm) nanoeukaryotes (D) and cyanobacteria (E) as a function of time. Each symbol represents the mean \pm range of duplicate samples; no error bars indicate the errors are smaller than the width of the symbol.

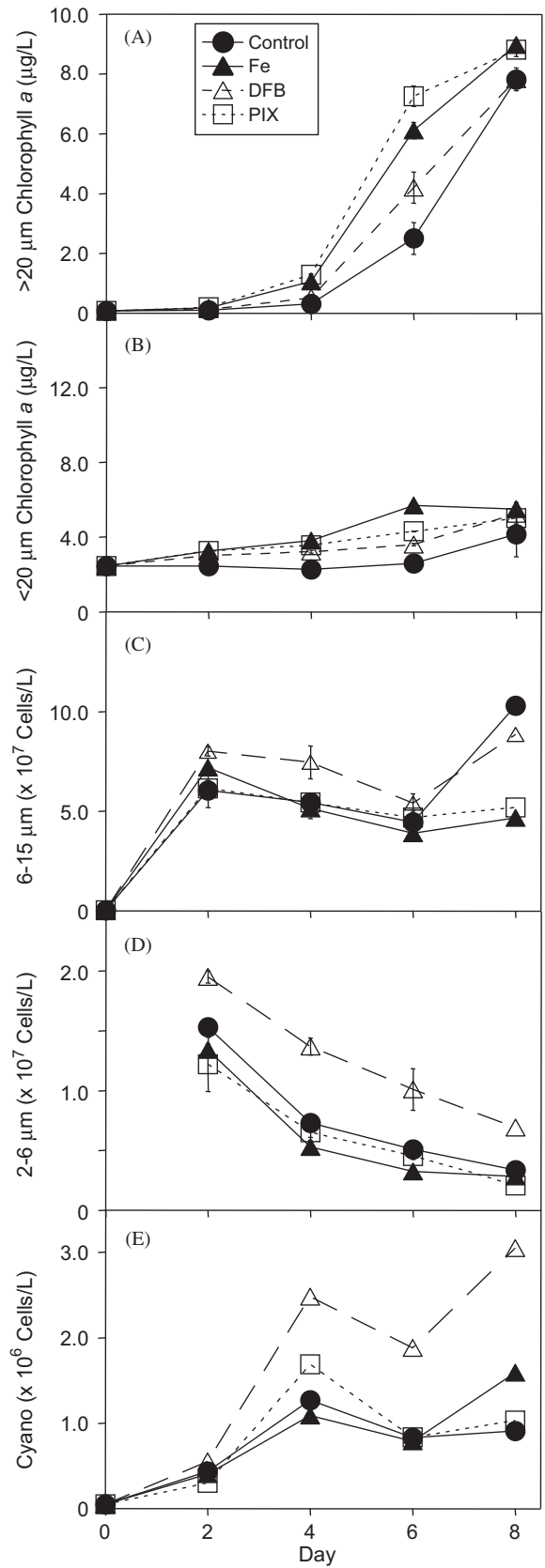


Fig. 4. The size-fractionated growth response to iron and Fe(III)-ligand amendments during the Middle Bloom experiment (August 4, 2004) for >20- μm phytoplankton (A), <20- μm phytoplankton (B), large (6–15 μm) nanoeukaryotes (C), small (2–6 μm) nanoeukaryotes (D), and cyanobacteria (E) as a function of time. Each symbol represents the mean \pm range of duplicate samples; no error bars indicate the errors are smaller than the width of the symbol.

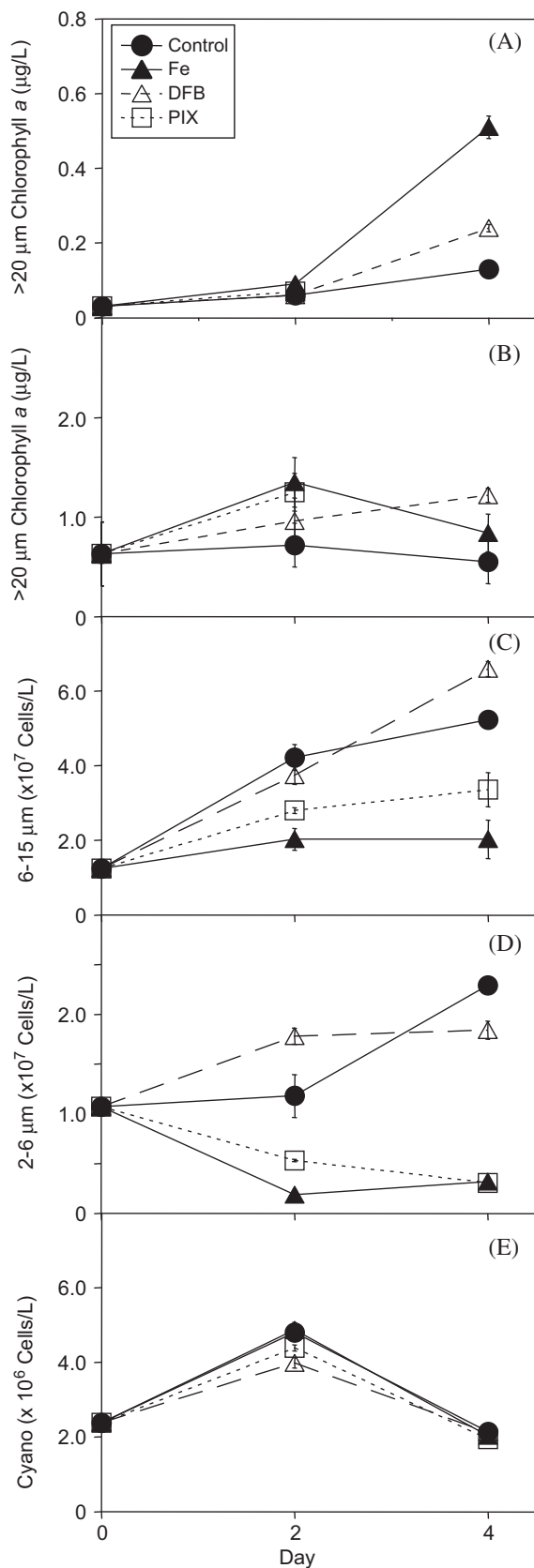


Fig. 5. The size-fractionated growth response to iron and Fe(III)-ligand amendments during the Late Bloom experiment (August 13, 2004) for >20- μm phytoplankton (A), <20- μm phytoplankton (B), large (6–15 μm) nanoeukaryotes (C), small (2–6 μm) nanoeukaryotes (D), and cyanobacteria (E) as a function of time. Each symbol represents the mean \pm range of duplicate samples; no error bars indicate the errors are smaller than the width of the symbol.

less ($p < 0.05$, LMMC) than in the control (Fig. 3C). The relative effect of Fe(III) on the small nanoeukaryotes (2–6 μm) appeared to be similar to that of large nanoeukaryotes, though these data are incomplete due to instrument problems (Fig. 3D). In contrast, cyanobacteria abundance increased substantially in both the control and the Fe(III) treatment of the Middle Bloom incubation, with the added iron having no effect on net growth (Fig. 4E). The small nanoeukaryotes (2–6 μm) decreased uniformly across all treatments in the Middle Bloom experiment ($p < 0.001$, linear mixed model Day term contrast; Fig. 4D) while large nanoeukaryotes (6–15 μm) also showed no effect from added Fe(III); cell numbers increased sharply by Day 2 but then remained constant over time in both the control and the Fe(III) treatment (Fig. 4C). Fe(III) addition also had no effect on cyanobacteria abundance in the Late Bloom experiment (Fig. 5E), but showed a negative effect on the numbers of small and large nanoeukaryotes relative to their respective controls ($p < 0.001$ for both groups, LMMC; Fig. 5C, D).

The effect of adding more iron to the fertilized patch waters appeared to be more uniform for the microphytoplankton (>20 μm). Chlorophyll *a* concentrations of the Early Bloom Fe(III) treatment increased above control values by Day 6 to roughly twice that in the controls by Day 8 (Fig. 3A), corresponding to $\sim 25\%$ higher growth rates ($1.27 \pm 0.05 \text{ d}^{-1}$ vs. $1.02 \pm 0.07 \text{ d}^{-1}$) and the effect of iron was significant in the statistical model ($p < 0.05$, LMMC). Fe(III) addition in the Middle Bloom experiment increased microphytoplankton chlorophyll *a* concentrations by ~ 3 -fold over those in the controls by Day 6, raising growth rates by 35% relative to the control ($0.81 \pm 0.12 \text{ d}^{-1}$ to $1.09 \pm 0.01 \text{ d}^{-1}$), although a subsequent growth surge in the control bottles narrowed this difference (Fig. 4A). The stimulatory effect of Fe(III) addition on microphytoplankton chlorophyll *a* was only marginally significant ($p = 0.09$, LMMC) in the Middle Bloom experiment when all days were considered, but the effect of Fe(III) became highly significant ($p < 0.005$, LMMC) when the last observations were not included in the model. Similarly, Fe(III) addition to fertilized patch waters near the end of the SEEDS II bloom increased microphytoplankton chlorophyll *a* concentrations by ~ 4 -fold in the large (> 20 μm) size fraction ($p < 0.001$, LMMC; Fig. 5A), doubling net growth rates from $0.55 \pm 0.12 \text{ d}^{-1}$ to $1.04 \pm 0.09 \text{ d}^{-1}$.

There are no equivalent cell number data for the large eukaryotes (> 15 μm) because the dominant chain-forming diatoms were not compatible with flow cytometric analysis. Qualitative microscopic analyses on-board ship verified that large diatoms dominated the large size fraction and that cell abundances were much higher in the Fe(III) treatment than in the control. In short then, supplementing the fertilized patch waters with substantially more iron (3 nM Fe(III)) enhanced both diatom growth rates and biomass accumulation throughout the entire *in situ* bloom trajectory.

The drawdown rates of macronutrients were consistent with the pattern of phytoplankton biomass changes in each of the three experiments (Table 1), with Fe(III) addition increasing nitrate+nitrite, silicate, and phosphate utilization rates in the Early Bloom experiment by 47%, 49%, and 54%, respectively (Fig. 6). Even so, Si:N drawdown ratios were 0.9 in both the control and the Fe(III) treatment, suggesting that iron additions did not alter the degree of frustule silicification in the growing diatoms. Fe(III) addition also increased nutrient drawdown rates in the Middle Bloom experiment (nitrate+nitrite, 46%; silicate, 73%; phosphate, 140%) (Fig. 6). However, Si:N drawdown increased from 1.1 in the controls to 1.4 in the Fe(III) treatment in this experiment (Table 1), perhaps indicating a higher proportional rate of Si utilization (i.e., increased diatom dominance). Only minimal nutrient drawdown occurred during the abbreviated Late Bloom experiment, although the Fe(III) treatment did show the largest drawdown of nitrate+nitrite (Fig. 6).

3.3. Ligand effects on phytoplankton growth responses

The effect of Fe(III)-complexing ligands on the growth response of in-patch phytoplankton was measured to assess whether organic complexation would mediate Fe availability. Protoporphyrin IX (PIX) was chosen as a potential analog for the comparatively weaker ligand class (L_2), while the siderophore desferrioximine B (DFB) was used to represent a stronger ligand class (L_1). Adding premixtures of these comparatively strong (DFB) and weak (PIX) Fe(III) ligand complexes had mixed effects on altering iron availability to in-patch phytoplankton. The addition of Fe(III)-PIX significantly increased the phytoplankton community biomass (measured on GF/F) in the Middle Bloom ($p < 0.05$, LMMC) and the Late Bloom ($p < 0.01$, LMMC) experiments (data not shown but represented as the sum of Figs. 4A+B and 5A+B). The addition of Fe(III)-DFB had no effect on the change in phytoplankton community biomass in the Early and Middle Bloom experiments though it did increase the community

Table 1
Nutrient utilization in the Early, Middle and Late Bloom deckboard incubation experiments.^a

Drawdown rates ($\mu\text{M}/\text{d}$)	Control	Fe(III)	Fe(III)-PIX	Fe(III)-DFB
<i>Early bloom experiment</i>				
N	3.4	5.0	4.4	3.7
Si	3.7	5.5	4.7	3.8
P	0.20	0.32	0.3	0.2
Si:N	0.9	0.9	0.8	0.8
<i>Middle bloom experiment</i>				
N	2.0	3.0	3.0	2.7
Si	2.3	4.0	3.6	2.7
P	0.13	0.29	0.1	0.1
Si:N	1.1	1.4	1.3	1.0
<i>Late bloom experiment</i>				
N	0.1	0.7	0.3	0.6
Si	-0.7	-0.5	-0.5	-0.4
P	0.0	0.0	0.0	0.0
Si:N	-5.6	-0.6	-1.9	-0.8

The negative drawdown rates for Si in the Late Bloom Experiment may be due to enhanced Si remineralization by bacteria in the bottles. See Kudo et al. (2009) for discussion on bacterial abundance and activity during SEEDS II.

^a N denotes the sum of $\text{NO}_3^- + \text{NO}_2^-$ but does not include reduced nitrogen substrates.

biomass in the Late Bloom experiment ($p < 0.01$, LMMC), but to a significantly lesser extent than the Fe(III) and Fe(III)-PIX treatments ($p < 0.05$, LMMC). Both ligands had little apparent effect on iron availability to the small size fraction ($< 20 \mu\text{m}$) during the Early Bloom incubation (Fig. 3B), and differences in the Late Bloom incubation for this size fraction were too small to assess the availability of these iron species relative to each other or to inorganic iron (Fig. 5B). However, both complexed forms of iron did slightly enhance the net growth of small ($< 20 \mu\text{m}$) phytoplankton in the Middle Bloom incubation, although apparently neither Fe(III)-DFB nor Fe(III)-PIX was as available as inorganic Fe(III) (Fig. 4B).

The effects of Fe(III)-PIX and Fe(III)-DFB on iron availability to the large ($> 20 \mu\text{m}$) size fraction were more uniform in the patch community as the SEEDS II bloom evolved. Fe(III)-DFB was poorly available to diatoms relative to inorganic iron additions in all three incubation experiments. Even so, growth rates in the DFB treatments of the three experiments were slightly greater ($\sim 0.2 \text{ d}^{-1}$) than in their respective controls, which was statistically significant in the Early Bloom experiment ($p < 0.02$, LMMC; Fig. 3A). The apparently enhanced growth in DFB treatments in each case occurred in latter stages of the incubations (Figs. 3A, 4A, and 5A), when the potential contributions of recycled iron (i.e., the release of intracellular iron—Hutchins and Bruland, 1994) complicate interpretations.

Flow cytometric data showed that Fe(III)-PIX generated essentially the same growth response as in the control and Fe(III) treatment for the cyanobacteria and small and large nanoeukaryotes in the Early and Middle Bloom incubations. In the Late Bloom experiment, Fe(III)-DFB had a positive effect on large nanoeukaryotes ($6\text{--}15 \mu\text{m}$) abundance while both Fe and Fe(III)-PIX had a negative effect on cell abundance ($p < 0.05$; Fig. 5C). Similarly, the abundance of small nanoeukaryotes in the Late Bloom experiment decreased in both the Fe and the Fe(III)-PIX treatments ($p < 0.001$; Fig. 5D).

In contrast to siderophore-complexed iron, Fe(III)-PIX ligand mixture was readily available to the large ($> 20 \mu\text{m}$) phytoplankton, significantly increasing growth relative to the controls in the Early ($p < 0.01$, LMMC; Fig. 3A) and Middle ($p < 0.04$, LMMC; Fig. 4A) experiments. The statistical significance of the positive effect of Fe(III)-PIX increases ($p < 0.0005$, LMMC) when the growth surge in the controls over the final 2 days are not considered. The final day Fe(III)-PIX samples in the Late Bloom experiment

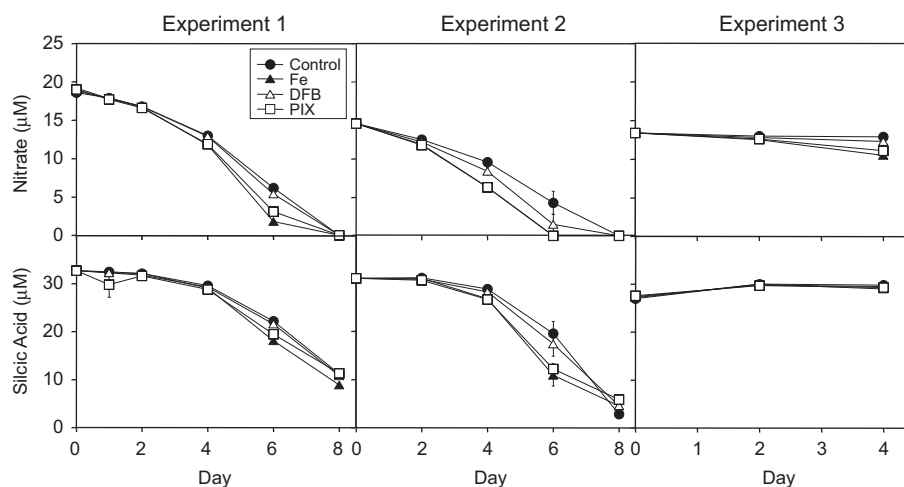


Fig. 6. Nitrate+nitrite (upper panels) and silicic acid (lower panels) concentration as a function of time in the Early (July 26, 2004), Middle (August 4, 2004) and Late Bloom (August 13, 2004) deckboard incubation experiments. Each symbol represents the mean \pm range of duplicate incubation samples; no error bars indicate the errors are smaller than the width of the symbol.

are not available due to an accident, which prevents assessment of whether this pattern of high availability continued as the fertilized patch community returned towards pre-bloom conditions.

Nutrient drawdown rates again were consistent with the patterns of biomass changes in these cultures. Utilization of nitrite+nitrate, silicate, and phosphate in the Fe(III)-PIX treatments closely followed that measured in the inorganic iron treatments, while the drawdown in Fe(III)-DFB treatments were intermediate with that of the controls (Fig. 6). As a consequence, Si:N drawdown ratios in the Fe(III)-PIX treatments were within the error of that in the inorganic Fe(III) treatments, while those in the Fe(III)-DFB treatments were closer to that measured in the controls (Table 1).

4. Discussion

The overall phytoplankton growth response to iron addition in SEEDS II was dramatically less than recorded during SEEDS I (Tsuda et al., 2003), despite having a second iron infusion after 6 days. Understanding the fundamental reasons for the great disparity in outcomes between these replicate experiments in the same HNLC location is essential to forecasting how variable iron supply influences ecosystem structure and carbon export from surface waters. Evidence from copepod feeding rate experiments suggest the proximate reason for the smaller SEEDS II response was that copepod grazing held the diatoms in check (Saito et al., 2009; Tsuda et al., 2007); an unexpected outcome if diatoms were growing optimally. Deckboard incubation experiments were used here to assess the iron nutritional status of the patch community over time, and to investigate whether pulsed iron supply or modification of the chemical form of iron, as might occur during prolonged dust events, might alter the trajectory of the phytoplankton community response. Post-incubation fractionation of the community enabled us to examine separately the response of diatoms (>20- μm fraction), and hence potentially higher carbon export potential, and the pico and nanoplanktonic organisms (<20- μm fraction) having slower potential carbon export rates. Even so, an important caveat to these interpretations is that species composition in the patch changed over time (Suzuki et al., 2009; Tsuda et al., 2007) in ways that might not occur with sustained iron inputs. The findings here then provide good insight into factors responsible for the muted ecosystem response during SEEDS II, but may not be fully representative of the outcomes of longer-term natural iron fertilization events.

Although total phytoplankton growth rates in our incubation experiments were close to estimates of *in situ* growth from dilution experiments (Tsuda et al., 2009), total chlorophyll biomass was substantially higher in our bottle experiments. There also was nearly complete drawdown of macronutrients in these deckboard experiments (Fig. 6), signifying that conditions in the bottle experiments were more optimal than realized *in situ* within the SEEDS II-fertilized patch. The enhanced growth in the controls was size related, with diatom growth (>20 μm) in the Early Bloom incubation controls (1.0d^{-1}) ~3-fold greater than net growth rates in the smaller size fraction (0.30d^{-1}), and these differences were an order of magnitude larger for the Middle Bloom experiment (0.81 vs. 0.02d^{-1} , >20 μm :<20 μm). There was no major increase in the biomass in the controls of the Late Bloom experiment, though the growth rates of the >20- μm size fraction were ~4-fold higher than the <20- μm size fraction (0.55 vs. 0.1d^{-1} , respectively). In each case then, while the overall phytoplankton growth rates in the bottles were similar to that *in situ*, the diatoms consistently grew faster in the bottles.

There are at least three possible factors that may have enhanced diatom growth in the control bottles. Iron contamination effects always are the initial concern, but spot measurements conducted on-board by flow injection analysis indicate no iron contamination in these experiments. Alternatively, reduced grazing pressure in the bottles likely played some role in the higher phytoplankton cell yields. Saito et al. (2009) found grazing pressure by mesozooplankton to be a dominant factor in regulating the *in situ* diatom response during SEEDS II, but these grazers were largely excluded from our experiments by the 200- μm Nitex screening used when filling the culture vessels. Photochemical effects on iron speciation also likely contributed to the enhanced diatom growth by increasing the proportion of ambient iron in the bottles that was available to the diatoms. Roy and Wells (2008) found that a major fraction ($\geq 35\%$) of dissolved iron occurred as Fe(II) during daylight hours in both out-patch and in-patch surface waters, indicative of high photochemical cycling rates. The UV-dependent photoreduction rates would be intensified in the deckboard experiments exposed to 50% surface PPF (despite attenuation by neutral density screening and partial UV absorption by the polycarbonate bottles). Photochemical cycling is believed to increase iron availability by sustaining elevated “steady-state” concentrations of inorganic iron (Rue and Bruland, 1997; Sunda, 2002; Wells et al., 1991). Indeed, encapsulating bottles with UV filters in deckboard experiments markedly decreases the phytoplankton growth response to low-level iron additions in the eastern subarctic Pacific (Wells et al., unpublished data). In any event, while it is instructive to consider the possible complications arising from decreased grazing pressure and increased photochemical cycling, these effects were uniform among the incubation treatments and do not impact our ability to test the primary question of whether persistent iron limitation contributed to the comparatively small ecosystem response observed during SEEDS II.

The rate of nitrate+nitrite drawdown decreased in controls of the successive experiments as the phytoplankton community in the patch changed over time, reflecting a return to iron limitation (Fig. 6). In contrast, silicate drawdown increased from the Early to Middle Bloom incubations leading to a small increase in Si:N drawdown ratio (0.9 to 1.1). Drawdown ratios approximating unity normally indicate iron-replete conditions, while higher ratios (>1.5) reflect iron limitation (Hutchins and Bruland, 1998; Takeda, 1998). However, diatoms likely accounted for too small a proportion of total nitrate uptake here to reflect this trend. Indeed, the Si:N drawdown ratio fell below zero in the Late Bloom incubation indicative of the small proportional growth attributable to diatoms (Fig. 5; Table 1).

Iron limitation was a primary and consistent factor restricting the growth rates of diatoms within the SEEDS II iron-fertilized patch (Figs. 3A, 4A, 5A) even though total dissolved iron concentrations (~0.7 nM, Early Bloom; ~0.4 nM, Middle Bloom; 0.3 nM, Late Bloom; Nishioka et al., 2009) remained well above diffusion-limited thresholds for unrestricted diatom growth (Hudson and Morel, 1990; Wells, 2003). The relative increase in the biomass response associated with the large- and small-sized fractions varied dramatically over the SEEDS II bloom trajectory as a result of alleviation of iron limitation (Fig. 7). Chlorophyll *a* biomass in the large (>20 μm) size fraction increased progressively (relative to the control) from ~100% early in the mesoscale bloom to 300% late in the SEEDS II bloom, though the absolute increase in the Late Bloom incubation was small. In all cases, the *in situ* microplanktonic community remained iron limited, despite the two in-patch iron infusions. Maximum chlorophyll *a* concentrations in the deckboard Fe(III)-enrichment treatments reached an order of magnitude higher than the observed *in situ* chlorophyll *a* concentrations (Fig. 1), indicating

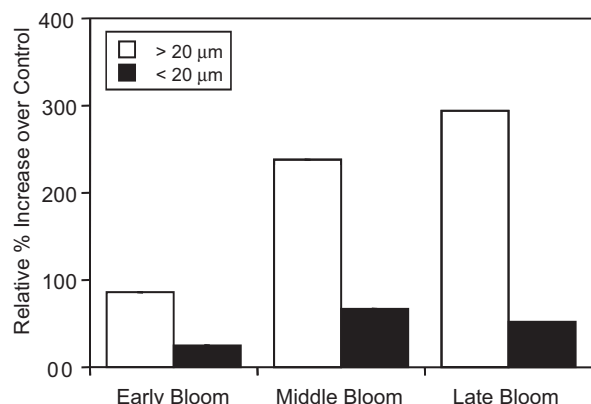


Fig. 7. The relative percent increase in chlorophyll biomass in the small (<20- μm) and large (>20- μm) size fractions with iron addition over that in the respective controls on Day 4 of the Early, Middle and Late Bloom incubation experiments.

that the main factor continuing to limit microphytoplankton in the patch was persistently low iron availability, despite the elevated dissolved iron concentrations measured (Kondo et al., 2008). The effect of Fe(III) amendment on the <20 μm size fraction is more muted, though substantial increases (~50% over the controls) also were observed (Fig. 7). The iron limitation of diatoms demonstrated here would have contributed substantially to the importance of grazing regulation of the *in situ* diatom growth response.

Iron speciation in the patch was overwhelmingly controlled by complexation with strong organic ligands (Kondo et al., 2008), as observed in earlier mesoscale iron-enrichment studies (Croft et al., 2001; Rue and Bruland, 1997; Takeda et al., 2002), and it appears that these ligand complexes restricted iron availability to diatoms (see below). The additions of 3 nM Fe(III) exceeded the free ligand concentrations (Kondo et al., 2008) and increased chlorophyll *a* concentrations over the controls by ~90%, 240%, and 300% in the Early, Middle, and Late Bloom incubations, respectively (Fig. 7). The progressively greater effect with time since fertilization presumably reflects increasing iron stress as dissolved iron concentrations decreased in the patch (Nishioka et al., 2009). Thus while mesozooplankton grazing on diatoms indeed was a major factor regulating the magnitude of the diatom response *in situ* during SEEDS II (Tsuda et al., 2007), our findings suggest that grazing control was effective only because diatom growth rates were restricted by continued iron limitation. It is worth noting that the average light intensity in our experiments (50% surface irradiance) was greater than the average irradiance within the mixed layer, which would tend to decrease cellular Fe demand within the cultures (Sunda and Huntsman, 1998). It is possible then that iron limitation effects in-patch waters were even greater than indicated in our findings.

In contrast to the diatoms, iron additions did not enhance cell numbers of cyanobacteria and small and large nanoeukaryotes. Moreover, the large nanoeukaryotes grew better in the control bottles than the iron treatments in the Early and Late Bloom experiments, and a similar iron inhibition effect was observed for the small nanoeukaryotes in the Late Bloom experiment (Figs. 3–5). This result is opposite to that observed in the chlorophyll data, where <20 μm chlorophyll *a* concentrations increased with added Fe relative to the controls by ~25%, ~70%, and ~50% by Day 4 in the Early, Middle and Late Bloom incubations, respectively (Fig. 7). The increase in <20 μm chlorophyll *a* concentrations in the Fe(III) and Fe(III)-PIX treatments thus suggest changes in cell physiology, or shifts in species composition, rather than increases in cell numbers, in contrast to the >20- μm size fraction where shipboard qualitative micro-

scopic observations showed higher diatom abundance. These combined findings indicate that pico- and nanoplankton in our incubations likely were co-limited by iron and grazing by an active micrograzer community in the bottles, similar to that observed *in situ* in the fertilized patch (Tsuda et al., 2009).

The addition of the Fe(III)-DFB complex had little positive effect for the most part on the chlorophyll biomass of microphytoplankton (>20 μm) (Figs. 3–5). These findings show that diatoms have a poor ability to access iron in a hydroxamate-type siderophore; a functional group identified to be a constituent in the strong class of Fe(III)-complexing ligands in seawater (Macrellis et al., 2001). A large proportion of iron in the patch existed in similarly strong complexes (Kondo et al., 2008) and though the specific nature of these strong ligands remains unknown, the findings here suggest that organic complexation would have been a primary factor limiting the diatom growth response in SEEDS II.

The apparent availability of Fe(III)-DFB to diatoms (>20 μm) increased slightly during the latter stages of each incubation experiment (Figs. 3A, 4A, 5A), as has been observed in coastal waters off Washington State and California (Trick et al., unpublished data). It is possible that this change reflects low-level cellular adaptation to utilize this Fe(III) complex, perhaps through induction of high-affinity iron uptake systems that cause reductive release of iron from strong Fe(III) complexes (Maldonado et al., 2004; Maldonado and Price, 1999; Wells et al., 2005). But if so, then why would diatoms be less successful adapting to utilize the ambient pool of Fe(III)-ligand complexes? One reason may be that they lacked sufficient copper availability to activate these high-affinity systems, as indicated in earlier studies in iron-limited coastal waters populated by pennate diatoms (Wells et al., 2005) as well as separate studies conducted during SEEDS-II (Trick et al., unpublished data).

Other factors also may have contributed to the apparent time-dependent change in Fe(III)-DFB availability in these cultures. For example, Hutchins and Bruland (1994) showed in an elegant series of experiments that the growth of eukaryotic phytoplankton in cultures of natural phytoplankton assemblages was supported by (recycled) iron added initially in the form of prokaryotic cells. If indeed prokaryotic cells have the ability to utilize Fe(III)-DFB, as indicated here (see below) and reported elsewhere (Hutchins et al., 1999b), grazing and other processes ultimately would release this iron back to the dissolved phase complexed to metabolic debris. Regenerated iron is believed to be more available because the conditional constants of intracellular metabolites are lower than that of siderophore molecules (Hutchins et al., 1999b), consistent with the stimulation of growth by Fe-PIX shown in this study. Regeneration would become more significant as grazing progressed, consistent with the growth trends observed here. Regardless, the results show that Fe(III)-DFB availability to diatoms in these HNLC waters was substantially less than inorganic iron, consistent with findings from equatorial Pacific HNLC waters (Wells et al., 1994).

Addition of Fe(III)-DFB did significantly increase the abundance of cyanobacteria and to a lesser extent the abundance of large nanoeukaryotes (6–15 μm) in the Middle Bloom experiment (Fig. 4C, E) and also increased the abundance (Fig. 5C) and average forward scatter value (FSV: a measure of cell size) of large nanoeukaryotes in the Late Bloom experiment (FSV data not shown). These positive responses to Fe(III)-DFB in the nanoeukaryotes and cyanobacteria in the Middle and Late Bloom experiments contrasted with no positive response to Fe(III)-DFB in the >20- μm chlorophyll *a* fraction. In the opposite manner, the positive responses of the >20 μm -fraction to Fe(III) addition in the Early and Late Bloom experiments corresponded with significant negative responses in large nanoeukaryotic abundance.

The combination of these two inverse relationships between $>20\text{-}\mu\text{m}$ chlorophyll *a* and the abundance of nanoeukaryotes and cyanobacteria suggests that changes in iron complexation resulted in shifting competitive dominance of different components of the phytoplankton community. While addition of Fe(III) or Fe(III)-PIX yielded a competitive advantage to the diatoms, addition of Fe(III)-DFB increased their relative Fe-limitation, enabling nanoeukaryotes and cyanobacteria to out-compete the diatoms for nutrients and light. This effect was not observed in the Early Bloom experiment, when iron would have been less limiting, but as iron concentrations in the patch decreased the balance shifted and the addition of Fe(III)-DFB was sufficient to encourage the nanoeukaryotes and cyanobacteria at the expense of the larger diatoms in the Middle and Late Bloom experiments.

As noted above, the mixture of Fe(III) with PIX was readily available to diatoms, supporting optimal growth in both the Early and the Middle Bloom incubations (Figs. 3A and 4A). This finding is consistent with that reported by Hutchins et al. (1999b); however, contrary to earlier suggestions, there is evidence that PIX may not effectively complex Fe(III) under normal seawater conditions (Hopkinson et al., 2005; Rijkenberg et al., 2006). If so, then the Fe(III)-PIX treatment would be chemically similar to the inorganic Fe(III) treatment. Certainly the Fe(III)-PIX treatments tended to replicate the inorganic iron treatments and we have obtained similar results with phaeophorbide, another metabolic degradation product (Pickell et al., unpublished). However, the growth response of diatoms with Fe(III)-PIX was lower in the Early Bloom incubations (Fig. 3B), and the same was true for the small phytoplankton populations in the Middle Bloom experiment (Fig. 4B), indicating that PIX indeed had some measurable effect on iron speciation in these cultures. Rijkenberg et al. (2006) found that PIX adequately complexed photo-produced Fe(II) when both were added at elevated concentrations to open-ocean seawater. A major fraction of dissolved iron in surface waters of the HNLC region of SEEDS II existed as Fe(II) during daylight hours (Roy and Wells, 2008), and it is expected the same would be true in the culture vessels used for these experiments. If so, then PIX may have restricted iron availability in those few instances by stabilizing Fe(II), thereby interfering with the photochemical cycling of iron that is expected to facilitate iron availability to eukaryotic phytoplankton.

The Si:N drawdown ratios were similar among controls and treatments in the Early Bloom experiment (Table 1). The enhanced growth of diatoms in the Fe(III) and Fe(III)-PIX treatments, seen both in increased chlorophyll concentrations (Fig. 3) and in nutrient drawdown rates relative to controls (Table 1), is not reflected in a change in the uptake ratio of silicic acid to nitrate among the treatments (Fig. 6). Iron additions in SEEDS II greatly enhanced nitrate uptake rates in the patch (Kudo et al., 2009), as observed in previous mesoscale and deckboard experiments in other HNLC regions (e.g., see review by Cochlan, 2008). This increased uptake appears to have been matched by increased Si uptake in our incubation experiment, indicating diatoms were maintaining balanced growth. In contrast, addition of Fe(III) and Fe(III)-PIX in the Middle Bloom experiment led to slower rates of NO_3^- and Si(OH)_4 utilization (Table 1), but a substantial increase in $\text{Si(OH)}_4:\text{NO}_3^-$ drawdown ratios (>1.3) relative to the control and Fe(III)-DFB (~ 1.0) (Table 1), an opposite trend to what may be expected when iron becomes more available. However, this utilization ratio does not consider the increased use of ammonium by phytoplankton as this regenerated N source presumably became increasingly available *in situ* from the markedly enhanced zooplankton remineralization occurring during the middle stage of the SEEDS II experiment (Kudo et al., 2009; Saito et al., 2009).

The findings here demonstrate that the microphytoplankton (diatom) growth response in the SEEDS II experiment, although significant relative to conditions outside the fertilized patch, remained sharply curtailed by persistent iron limitation. This limitation occurred even though dissolved iron concentrations in the patch exceeded the diffusion-limited threshold for rapid growth of pennate diatoms (Hudson and Morel, 1993; Wells, 2003). Measurements have shown that Fe(III) speciation was overwhelmingly controlled by strong organic complexation (Kondo et al., 2008); iron forms shown here to likely be poorly available to diatoms. The growth that did occur may have resulted from a sub-fraction of the iron occurring in weaker ligands, which did support diatom growth in our experiments, or from the photo-reductive release of Fe(II) from Fe(III) complexes, a process that maintained elevated ($>100\text{ pM}$) concentrations of Fe(II) species in the patch during daylight hours (Roy and Wells, 2008). The resulting suboptimal diatom growth rates would have increased the relative importance of mesozooplankton grazing as a factor controlling the microphytoplankton community trajectory, and may account for the large difference between the ecosystem responses observed in SEEDS I and SEEDS II mesoscale fertilization experiments.

Acknowledgements

This research was supported by NSF Grants OCE-0241752 (Wells) and OCE-0241385 (Cochlan), NSERC Discovery Grant (Trick), and by the Office of Science (BER), US Department of Energy Grant no. DE-FG02-02ER63429 (Wells and Trick) and DE-FG02-02ER63430 (Cochlan). We express our deep appreciation to Drs. A. Tsuda and S. Takeda and their numerous colleagues for their generous invitation to participate in the SEEDS II mesoscale Fe-enrichment experiment. We thank the Captain and crew of the R/V *Kilo Moana* for their help during this challenging experiment. This work would not have been possible without the excellent support of many individuals including Julian Herndon (RTC/SFSU), Julia Betts (RTC/SFSU), Denis Costello (Teacher at Sea, North High School, Torrance CA), Lisa Pickell (U.Maine), Eric Roy (U.Maine), Amanda Burke (U.Maine), Katrina Iglie (UWO), and Fadi Hamadani (UWO).

References

- Barbeau, K., Rue, E.L., Trick, C.G., Bruland, K.W., Butler, A., 2003. Photochemical reactivity of siderophores produced by marine heterotrophic bacteria and cyanobacteria by characteristic Fe(III) binding groups. *Limnology and Oceanography* 48, 1069–1073.
- Berg, C.M.G.V.D., 1995. Evidence for organic complexation of iron in seawater. *Marine Chemistry* 50 (1), 139–157.
- Blain, S., Treguer, P., Belviso, S., Bucciarelli, E., Denis, M., Desabre, S., Fiala, M., Jezequel, V.M., Le Fevre, J., Mayzaud, P., Marty, J.C., Razouls, S., 2001. A biogeochemical study of the island mass effect in the context of the iron hypothesis: Kerguelen Islands, Southern Ocean. *Deep-Sea Research I-Oceanographic Research Papers* 48 (1), 163–187.
- Boyd, P.W., Jickells, T., Law, C.S., Blain, S., Boyle, E.A., Buesseler, K.O., Coale, K.H., Cullen, J.J., de Baar, H.J.W., Follows, M., Harvey, M., Lancelot, C., Levasseur, M., Owens, N.P.J., Pollard, R., Rivkin, R.B., Sarmiento, J., Schoemann, V., Smetacek, V., Takeda, S., Tsuda, A., Turner, S., Watson, A.J., 2007. Mesoscale Iron enrichment experiments 1993–2005: synthesis and future directions. *Science* 315 (5812), 612–617.
- Boyd, P.W., Muggli, D.L., Varela, D.E., Goldblatt, R.H., Chretien, R., Orians, K.J., Harrison, P.J., 1996. *In vitro* iron enrichment experiments in the NE subarctic Pacific. *Marine Ecology Progress Series* 136, 179–193.
- Coale, K.H., 1991. Effects of iron, manganese, copper, and zinc enrichments on productivity and biomass in the subarctic Pacific. *Limnology and Oceanography* 36 (8), 1851–1864.
- Coale, K.H., Johnson, K.S., Fitzwater, S.R., Gordon, R.M., Tanner, S., Chavez, F.P., Ferioli, L., Sakamoto, C., Rogers, P., Millero, F., Steinberg, S., Nightingale, P., Cooper, D., Cochlan, W.P., Landry, M.R., Constantinou, J., Rollwagin, G., Travnica, A., Kudela, R., 1996. A massive phytoplankton bloom induced by an

- ecosystem-scale iron fertilization experiment in the equatorial Pacific. *Nature* 383, 495–501.
- Cochlan, W.P., 2008. Nitrogen uptake in the Southern Ocean. In: Capone, D.G., Bronk, D.A., Mulholland, M.R., Carpenter, E.J. (Eds.), *Nitrogen in the Marine Environment*, 2nd Edition, Academic Press, Elsevier, pp. 569–596.
- Croot, P.L., Bowie, A.R., Frew, R.D., Maldonado, M.T., Hall, J.A., Safi, K.A., LaRoche, J., Boyd, P.W., Law, C.S., 2001. Retention of dissolved iron and Fe(II) in an iron induced Southern Ocean phytoplankton bloom. *Geophysical Research Letters* 28, 3425–3428.
- Croot, P.L., Johansson, M., 2000. Determination of iron speciation by cathodic stripping voltammetry in seawater using a competitive ligand 2-(2-Thiazolylazo)-p-cresol(TAC). *Electroanalysis* 12 (8), 565–576.
- Crumbliss, A.L., 1991. Aqueous solution equilibrium and kinetic studies of iron siderophore and model siderophore complexes. In: Winkelmann, G. (Ed.), *CRC Handbook of Microbial Iron Chelates*. CRC Press, NY (Chapter 7).
- Cullen, J.T., Berquist, B.A., Moffett, J.W., 2006. Thermodynamic characterization of the partitioning of iron between soluble and colloidal species in the Atlantic Ocean. *Marine Chemistry* 98 (2–4), 295–303.
- de Baar, H.J.W., Boyd, P.W., Coale, K., Landry, M.R., Tsuda, A., Assmy, P., Bakker, D.C.E., Bozec, Y., Barber, R.T., Brzezinski, M.A., Buessler, K.O., Boye, M., Croot, P.L., Gervais, F., Gorbunov, M.Y., Harrison, P.J., Hiscock, W.T., Laan, P., Lancelot, C., Law, C.S., Levasseur, M., Marchetti, A., Millero, F.J., Nishioka, J., Nojiri, Y., van Oijen, T., Riebesell, U., Rijkenberg, M.J.A., Saito, H., Takeda, S., Timmermanns, K.R., Veldhuis, M.J.W., Waite, A.M., Wong, C.-S., 2005. Synthesis of iron fertilization experiments: from the iron age to the age of enlightenment. *Journal of Geophysical Research* 110 (C09S16), 1–24.
- Gledhill, M., van den Berg, C.M.G., 1994. Determination of complexation of iron (III) with natural organic complexing ligands in seawater using cathodic stripping voltammetry. *Marine Chemistry* 47, 41–54.
- Hopkinson, B., Nunnery, J., Barbeau, K., 2005. Bioavailability and Chemistry of Iron(III)–Porphyrin Complexes. *American Chemical Society, ACS*.
- Hudson, R.J.M., Morel, F.M.M., 1990. Iron transport in marine phytoplankton: kinetics of cellular and medium coordination reactions. *Limnology and Oceanography* 35 (5), 1002–1020.
- Hudson, R.J.M., Morel, F.M.M., 1993. Trace metal transport by marine microorganisms: implications of metal coordination kinetics. *Deep-Sea Research* 40 (1), 129–150.
- Hutchins, D.A., Bruland, K.W., 1994. Grazer-mediated regeneration and assimilation of Fe, Zn and Mn from planktonic prey. *Marine Ecology Progress Series* 110, 259–269.
- Hutchins, D.A., Bruland, K.W., 1998. Iron-limited diatom growth and Si:N uptake ratios in a coastal upwelling regime. *Nature* 393, 561–564.
- Hutchins, D.A., Franck, V.M., Brzezinski, M.A., Bruland, K.W., 1999a. Inducing iron limitation in iron-replete coastal waters with a strong chelating ligand. *Limnology and Oceanography* 44, 1009–1018.
- Hutchins, D.A., Witter, A.E., Butler, A., Luther, G.W., 1999b. Competition among marine phytoplankton for different chelated iron species. *Nature* 400, 858–860.
- Knap, A., Michaels, A., Close, A., Ducklow, H., Dickson, A., 1996. Protocols for the Joint Global Ocean Flux Study (JGOFS) Core Measurements. In: 19, J.R.N. (Ed.), *Reprint of the Intergovernmental Oceanic Commission Manuals and Guides No. 29*. UNESCO, Bergen, p. 170.
- Knepel, K., Bogren, K. (Eds.), 2002. Determination of orthophosphate by flow injection analysis: QuikChem[®] Method 31-115-01-1-H. Lachat Instruments, Milwaukee, WI.
- Kondo, Y., Takeda, S., Nishioka, J., Obata, H., Furuya, K., Johnson, W.K., Wong, C.S., 2008. Organic iron (III) complexing ligands during an iron enrichment experiment in the western subarctic North Pacific. *Geophysical Research Letters* 35 (12), L12601.
- Kudo, I., Nori, Y., Cochlan, W.P., Suzuki, K., Aramaki, T., Ono, T., Nojiri, Y., 2009. Primary productivity, bacterial productivity and nitrogen uptake in response to iron enrichment assimilation during the SEEDS II. *Deep-Sea Research II* 56 (26), 2755–2766.
- Leblanc, K., Hare, C.E., Boyd, P.W., Bruland, K.W., Sohst, B., Pickmere, S., Lohan, M.C., Buck, K., Ellwood, M., Hutchins, D.A., 2005. Fe and Zn effects on the Si cycle and diatom community structure in two contrasting high and low-silicate HNLC areas. *Deep-Sea Research I-Oceanographic Research Papers* 52 (10), 1842–1864.
- Macrellis, H.M., Trick, C.G., Rue, E.L., Smith, G., Bruland, K.W., 2001. Collection and detection of natural iron-binding ligands from seawater. *Marine Chemistry* 76, 175–187.
- Maldonado, M.T., Chong, J., Leus, D., Karpenko, N., Harris, S., 2004. The role of copper in the high-affinity iron transport system of marine diatoms. *American Society of Limnology and Oceanography*, Honolulu, HI.
- Maldonado, M.T., Price, M.M., 1999. Utilization of iron bound to strong organic ligands by plankton communities in the subarctic Pacific Ocean. *Deep-Sea Research II* 46, 2447–2473.
- Marie, D., Partensky, F., Jacquet, S., Vaulot, D., 1997. Enumeration and cell cycle analysis of natural populations of marine picoplankton by flow cytometry using the nucleic acid stain SYBR Green I. *Applied Environmental Microbiology* 63 (1), 186–193.
- Martin, J.H., 1990. Glacial–interglacial CO₂ change: the iron hypothesis. *Paleoceanography* 5 (1), 1–13.
- Martin, J.H., Fitzwater, S.E., 1988. Iron deficiency limits phytoplankton growth in the North-East Pacific subarctic. *Nature* 331, 341–343.
- Martinez, J.S., Haygood, M.G., Butler, A., 2001. Identification of a natural desferrioxamine siderophore produced by a marine bacterium. *Limnology and Oceanography* 46, 420–424.
- Nishioka, J., Takeda, S., Konda, Y., Obata, H., Doi, T., Tsumune, D., Wong, C.S., Johnson, W.K., Sutherland, N., Tsuda, A., 2009. Changes in iron concentrations and bio-availability during an open-ocean mesoscale iron-enrichment in the western subarctic Pacific, SEEDS II. *Deep-Sea Research II* 56 (26), 2796–2809.
- Powell, R.T., Donat, J.R., 2001. Organic complexation and speciation of iron in the South and Equatorial Atlantic. *Deep-Sea Research II Topical Studies in Oceanography* 48 (13), 2877–2893.
- Rijkenberg, M.J.A., Gerringa, L.J.A., Carolus, V.E., Velzeboer, I., Baar, H.J.W.d., 2006. Enhancement and inhibition of iron photoreduction by individual ligands in open ocean seawater. *Geochimica Cosmochimica Acta* 70 (11), 2790–2805.
- Roy, E., Wells, M.L., 2008. The persistence of Fe(II) in surface waters of the western subarctic Pacific. *Limnology and Oceanography* 53 (1), 89–98.
- Rue, E.L., Bruland, K.W., 1995. Complexation of Fe(III) by natural organic ligands in the central North Pacific as determined by a new competitive ligand equilibration adsorptive cathodic stripping voltammetric method. *Marine Chemistry* 50, 117–138.
- Rue, E.L., Bruland, K.W., 1997. The role of organic complexation on ambient iron chemistry in the equatorial Pacific Ocean and the response of a mesoscale iron addition experiment. *Limnology and Oceanography* 42, 901–910.
- Saito, H., Tsuda, A., Nojiri, Y., Aramaki, T., Ogawa, H., Yoshimura, T., Imai, K., Kudo, I., Nishioka, J., Ono, T., Suzuki, K., Takeda, S., 2009. Biogeochemical cycling of N and Si during the mesoscale iron-enrichment experiment in the western subarctic Pacific (SEEDS-II). *Deep-Sea Research II* 56 (26), 2852–2862.
- Salmon, T.P., Rose, A.L., Neilan, B.A., Waite, T.D., 2006. The FeL model of iron acquisition: nondissociative reduction of ferric complexes in the marine environment. *Limnology and Oceanography* 51 (4), 1744–1754.
- Shaked, Y., Kustka, A.B., Morel, F.M.M., 2005. A general kinetic model for iron acquisition by eukaryotic phytoplankton. *Limnology and Oceanography* 50 (3), 872–882.
- Smith, P., Bogren, K., 2001. Determination of nitrate and/or nitrite in brackish or seawater by flow injection analysis colorimeter: QuikChem Method 31-107-04-1-E. *Saline Methods of Analysis*. Lachat Instruments, Milwaukee, WI, 12pp.
- Sunda, W.G., 2001. Bioavailability and bioaccumulation of iron in the sea. In: Turner, D.R., Hunter, K.A. (Eds.), *The Biogeochemistry of Iron in Seawater*. Wiley, Chichester, pp. 41–84.
- Sunda, W.G., 2002. Bioavailability and bioaccumulation of iron in the sea. In: Turner, D.R., Hunter, K.A. (Eds.), *The Biogeochemistry of Iron in Seawater*. Wiley, New York.
- Sunda, W.G., Huntsman, S.A., 1998. Interrelated effects of iron, light and cell size on marine phytoplankton growth. *Nature* 390, 389–392.
- Suzuki, R., Ishimaru, T., 1990. An improved method for the determination of phytoplankton chlorophyll using N, N-dimethylformamide. *Journal of the Oceanographical Society of Japan* 46, 190.
- Suzuki, K., Saito, H., Isada, T., Hattori, A., Kiyosawa, H., Nishioka, J., Michael, R., McKay, L., Kuwata, A., Tsuda, A., 2009. Community structure and photosynthetic physiology of phytoplankton in the northwest subarctic Pacific during an in situ iron fertilization experiment (SEEDS II). *Deep-Sea Research II* 56 (26), 2733–2844.
- Takeda, S., 1998. Influence of iron availability on nutrient consumption ratio of diatoms in oceanic waters. *Nature* 393, 774–777.
- Takeda, S., Tsuda, A., Saito, H., Nojiri, Y., Nishioka, J., Kudo, I., Tsumune, D., 2002. Biogeochemical processes during the Subarctic Pacific Iron Experiment for Ecosystem Dynamics Study (SEEDS). *Ocean Sciences Meeting*, Honolulu, HI.
- Timmermanns, L.R., Gerringa, L.J.A., Baar, H.J.W.d., Wagt, B.V.d., Veldhuis, M.J.W., Jong, J.T.M.d., Croot, P.L., 2001. Growth rates of large and small Southern Ocean diatoms in relation to availability of iron in natural seawater. *Limnology and Oceanography* 46 (2), 260–266.
- Tsuda, A., Saito, H., Machida, R.J., Shimode, S., 2009. Meso- and microzooplankton responses to an in situ iron fertilization experiment (SEEDS-II) in the northwest subarctic Pacific. *Deep-Sea Research II* 56 (26), 2767–2778.
- Tsuda, A., Takeda, S., Saito, H., Nishioka, J., Kudo, I., Nojiri, Y., Suzuki, K., Uematsu, M., Wells, M.L., Tsumune, D., Yoshimura, T., Aono, T., Aramaki, T., Cochlan, W.P., Hayakawa, M., Imai, K., Isada, T., Iwanamoto, Y., Johnson, W., Kameyama, S., Kato, S., Kiyosawa, H., Kondo, Y., Levasseur, M., Machida, R., Nagao, Y., Nakagawa, F., Nakanishi, T., Nakatsuka, S., Narita, A., Noiri, Y., Obata, H., Ogawa, H., Oguma, K., Ono, T., Sakuragi, T., Sasakawa, M., Sato, M., Shimamoto, A., Takata, H., Trick, C.G., Watanabe, Y., Wong, C.-S., Yoshie, N., 2007. Evidence for the grazing hypothesis: grazing reduces phytoplankton responses of the HNLC ecosystem to iron enrichment in the western subarctic Pacific (SEEDS II). *Journal of Oceanography* 63, 983–994.
- Tsuda, A., Takeda, S., Saito, H., Nishioka, J., Nojiri, Y., Kudo, I., Kiyosawa, H., Shimamoto, A., Imai, K., Ono, T., Shimamoto, A., Tsumune, D., Yoshimura, T., Aono, T., Hinuma, A., Kinugasa, M., Suzuki, K., Sohrin, Y., Noiri, Y., Tani, H., Deguchi, Y., Tsurushima, N., Ogawa, H., Fukami, K., Kuma, K., Saino, T., 2003. A mesoscale iron enrichment in the Western subarctic Pacific induces a large centric diatom bloom. *Science* 300, 958–961.
- Wells, M.L., 1999. Manipulating iron availability in nearshore waters. *Limnology and Oceanography* 44, 1002–1008.
- Wells, M.L., 2003. The level of iron enrichment required to initiate diatoms blooms in HNLC waters. *Marine Chemistry* 82, 101–114.

- Wells, M.L., Mayer, L.M., Donard, O.F.X., de Souza Sierra, M.M., Ackleson, S., 1991. The photolysis of colloidal iron in the oceans. *Nature* 353, 248–250.
- Wells, M.L., Price, N.M., Bruland, K.W., 1994. Iron limitation and the cyanobacterium *Synechococcus* in equatorial Pacific waters. *Limnology and Oceanography* 39, 1481–1486.
- Wells, M.L., Trick, C.G., Cochlan, W.P., Hughes, P., Trainer, V.L., 2005. Domoic acid: the synergy of iron, copper and the toxicity of diatoms. *Limnology and Oceanography* 50 (6), 1908–1917.
- Welschmeyer, N.A., 1994. Fluorometric analysis of chlorophyll *a* in the presence of chlorophyll *b* and pheopigments. *Limnology and Oceanography* 39, 1985–1992.
- West, B.T., Welch, K.B., Galecki, A.T., 2007. *Linear Mixed Models*. Chapman & Hall, Boca Raton, FL.
- Witter, A.E., Lewis, B.L., Luther, G.W., 2000. Iron speciation in the Arabian Sea. *Deep-Sea Research II* 47, 1517–1539.
- Wolters, M., 2002. Determination of silicate in brackish or seawater by flow injection analysis. QuikChem[®] Method 31-114-27-1-D. Lachat Instruments, Milwaukee, WI, p. 12.